Polarization partition noise and intensity fluctuation linewidth in a nearly symmetric vector laser

S. Ciuchi* and M. San Miguel†
Instituto Mediterraneo de Estudios Avanzados, Censejo Superior de Investigaciones Científicas, Campus Universitat de les Illes Balears, E-07071 Palma de Mallorca, Spain

N. B. Abraham‡
Department of Physics, Bryn Mawr College, 101 North Merion Avenue, Bryn Mawr, Pennsylvania 19010-2899
(Received 20 May 1997)

We consider the statistical properties of the fluctuations in the orientation of the vector laser field for a nearly isotropic laser, addressing the competition between the randomizing influence of noise and the preference for linearly or circularly polarized emission induced by saturation in the laser medium and/or cavity anisotropies. We describe, through a nonperturbative analysis, a crossover regime from diffusion-induced polarization-isotropic emission to emission of nearly fixed polarization characteristics. In this crossover the linewidth of intensity fluctuations associated with one of the circularly polarized components of the vector field amplitude changes from decreasing to increasing with output power. This behavior can be expressed in terms of a single parameter that measures the pump or the total output intensity in terms of the ratio of the noise amplitude to the degree of cross saturation of the amplitudes of the circularly polarized components of the vector field amplitude. Analytical results are given for the linewidth of the intensity fluctuations. When the laser has a preference for linearly polarized emission, there is a weakly non-Lorentzian spectrum in the crossover region. When the laser has a ''preference'' for circularly polarized emission the crossover regime is characterized by a non-Lorentzian spectrum due to fast hopping between two circularly polarized eigenstates. We also describe ellipticity fluctuations induced by the diffusion of the direction of the main axis of the polarization ellipse in the presence of cavity birefringence. [S1050-2947(98)08202-X]

PACS number(s): 42.55.−f, 42.50.Lc

I. INTRODUCTION

The study of the selection of the polarization state of laser emission dates from the early days of laser physics [1,2] when most analyses of this question were formulated in terms of third-order Lamb theory [3]. Within that theoretical framework one derives coupled equations for the slowly varying amplitudes of the two orthogonal circularly polarized components of the electric field. A crucial parameter γ is the ratio of the cross saturation to the self-saturation of the field amplitudes. It depends on the field-material physics (including both the angular momentum of the states involved in the material transition and the decay rates of the different elements of the density matrix describing the material populations, dipoles, quadrupoles, and higher-order coherence terms). For weak coupling ($\gamma<1$) there is a preference for linearly polarized emission and for strong coupling ($\gamma>1$) there is a ''preference'' for circularly polarized emission. Marginal coupling ($\gamma=1$) leads to emission with arbitrary ellipticity and azimuth. Of course, the field-matter interaction is only one of several influences on the final polarization properties of a laser. Also crucial are cavity anisotropies (birefringence, dichroism, etc.). The saturable dispersion of the material transition is an additional important feature when there are phase-sensitive anisotropies (which introduce different optical frequency shifts, detunings, for differently polarized fields).

While studies of lasers with cylindrically symmetric geometries often focused on polarization properties [1,2,4], these considerations have not been common. Renewed theoretical and experimental interest in the polarization properties of laser light is associated with the role of the vectorial degree of freedom of the electric field in laser instabilities and dynamics in gas lasers, diode-pumped solid-state lasers, fiber lasers, optically pumped far-infrared lasers, and vertical cavity surface-emitting semiconductor lasers [5–24]. Satisfactory modeling of some of the dynamical behavior requires generalized Maxwell-Bloch equations or a modified form of field-population rate equations, either of which goes beyond third-order Lamb theory.

From the point of view of the statistical properties of laser light, the polarization state and the vector degree of freedom also add new features to the phase diffusion that contributes to the laser linewidth in a noise-driven conventional polarization-stabilized laser [25–32]. Lasers with different values for γ have their polarization properties affected differently by noise. The circularly polarized states are discrete, so noise causes either local fluctuations or hopping to the other state. By contrast, the linearly polarized states are a simply continuous family (in orientation angle) among which even weak noise can cause diffusion. The solutions of arbitrary elliptical polarization are a doubly countinuous family within which noise drives diffusion in both azimuth and ellipticity.

These features have been considered mostly a theoretical

*Permanent address: Dipartimento di Fisica Università de L'Aquila, I-67100 L'Aquila, Italy.
Electronic address: ciuchi@axscaq.aquila.infn.it
†Electronic address: maxi@hp1.uib.es
‡Electronic address: nabraham@brynmawr.edu

curiosity, since in most practical lasers there are some anisotropies that stabilize the emission on a particular polarization state. Most commonly the optical cavity is designed to minimize losses, typically by using Brewster-angled windows or material surfaces that lead to a well-stabilized linearly polarized emission. However, in addition to the relatively rare cylindrically symmetric geometries of early lasers, modern high-efficiency designs for solid-state lasers [using microchips [8] or vertical cavity surface-emitting lasers (VCSELs) [18]] may operate on a single spatial mode and often are not polarization stable. Since switching between distinct but differently polarized laser states often requires low holding power and extremely low switching energies, polarization could be a good property to choose for optical logic gates and signaling, making polarization fluctuations a matter of great concern for signal quality and performance degradation [19,33].

For gas lasers, where the material dynamics can be described more easily and more exactly, there have been recent experiments on small, high-gain, single-mode lasers to measure noise properties associated with fluctuations in the polarization state, such as polarization diffusion and its contribution to the laser's intensity linewidth [30,31]. In particular, polarization diffusion has been used, together with the Zeeman effect, as a practical method to measure the quantum-limited linewidth of a laser [32]. These results and potential applications call for further theoretical investigations.

In a conventional linearly polarized single-mode (SM) laser, even modestly above the lasing threshold, the intensity correlations decay very rapidly in time due to the strict confinement of the intensity around its stationary value. In contrast, the complex field amplitude has a slowly diffusing phase, driven by spontaneous emission noise. This causes the width of the spectrum of the intensity fluctuations to be much larger than the width of the field fluctuations. The intensity linewidth is proportional to the pumping rate, while the linewidth of the optical field, originating in the phase diffusion, is inversely proportional to the output power. Some modifications of these principles when the cavity linewidth approaches or exceeds the linewidth of the material transition have long been noted, but they were only more recently measured carefully [30].

The situation can be very different when there is competition between or among states of different polarization. The extreme case occurs for marginal coupling of the two circularly polarized components of the vector field, in which case there is no preferred polarization state for the lasing action. Such a polarization-symmetric (PS) laser in an ideal, polarization-symmetric cavity was considered by Graham [25,27]. The fluctuations of the intensity of any particular selected component of the emitted vector field are then correlated over very large times. This form of partition noise leads to an intensity linewidth that is inversely proportional to the pump rate. In the Poincaré representation of the polarization states [34] (see Fig. 1) the representative point of the laser vector field in this case performs a random walk on the surface of the Poincaré sphere, randomly visiting different elliptically polarized states. Noise leads to diffusion of the main axes (and of the ellipticity) of the polarization ellipse. This diffusion can be observed by measurements of the intensity-fluctuation correlation function of any polarized projection of the emission.

Far from the polarization-symmetric case, due either to anisotropic gain media or to cavity anisotropies, intensity correlations are those characteristic of a single-mode (polarized) laser [28]. However, the vectorial component of spontaneous emission noise perpendicular to the instantaneous direction of the vector laser electric field still causes polarization fluctuations.

From the preceding discussion it is clear that there should be an interesting crossover situation between the PS and SM behaviors when the value of γ is close enough to unity that the selection of a polarization state by field material or cavity anisotropy competes, with a similar strength, with the noise-induced tendency for diffusion over the entire surface of the Poincaré sphere. In this paper we analyze this crossover regime and describe the key differences in the crossover regimes between the situations when the cross-saturation parameter leads to a slight preference for linear or circular polarization. We find a crossover from decreasing to increasing intensity linewidth of one field component as the output power is increased. This crossover occurs well above threshold and should not be confused with the change of behavior that occurs for a single-mode laser when the laser is taken from slightly above threshold (where the noise contribution causes large percentage fluctuations in the total output intensity) to sufficiently far above threshold (where the noise contributes only very weak fluctuations to the total output intensity).

The experimental investigation of the crossover regime that we describe requires considering a nearly isotropic laser, that is, a laser with field-material interactions close to marginal coupling and small cavity anisotropies. From the point of view of the material gain anisotropies, possible gas lasers that might show this effect are those operating on [31] the $\lambda = 2.65$ and 2.03 μm lines of Xe, associated, respectively with $J = 1$ to 0 and $J = 1$ to 1 atomic transitions, and the $\lambda = 1.52$ and 3.3912 μm lines of Ne, which have $J = 1$ to 0 and $J = 1$ to 1 atomic transitions, respectively. These kinds of J to J' transitions are known to give marginal couplings except for the effects induced by atomic collisions [3,35–37].

Another laser in which these effects might be observed is the VCSEL. Within the model for polarization dynamics of VCSELs in Ref. [38] the effective coupling parameter depends sensitively on the carrier spin-flip relaxation rate. The coupling is close to marginal for fast relaxation [38,6]. The actual value of this parameter is the subject of current active research [39–41], but a situation close to marginal coupling seems possible. However, our treatment here of polarization partition noise is not directly applicable to VCSELs since we will restrict ourselves to a third-order Lamb theory, while VCSELs require a more involved description [5,6]. Still, some of the ideas put forth here may be helpful for understanding these devices. Concerning cavity anisotropies, we mention that there are now experimental techniques available to compensate and tune some of the unavoidable anisotropies. For example, a magnetic field can be used to compensate cavity anisotropies that otherwise select a direction of linear polarization [30–32] and intrinsic birefringence can be controlled [42] by localized stress. This opens the way to

studies of fluctuations in nearly isotropic lasers.

It is also possible that phenomena such as those discussed here could provide a useful benchmark for tests of commonly used models for semiconductor and solid-state multimode lasers that often both ignore the amplitude fluctuations (considering only intensities) and couple these modal intensities equally, via saturation, to the material inversion. Polarization dynamics in nearly polarization-isotropic lasers of these types might be a sensitive test of the assumption of neutral saturation coupling.

The problem considered in this paper has formal similarities to that of intensity correlations in two-mode lasers [43–45], both lasers with two longitudinal modes and lasers with two counterpropagating modes. The weak or strong coupling in those cases is associated with inhomogeneous and homogeneous broadening of the lasing transition, respectively. Many of the mathematical tools that we will use (for example, effective and average eigenvalues) were used for that problem [45] and the marginal coupling case was also mathematically discussed in this context. However, the crossover regime that we discuss for comparable cross-saturation asymmetry and noise strengths seems difficult to obtain (or maintain) in two-mode lasers. Despite the similarities, there is some difficulty both conceptually and practically with describing polarization fluctuations in terms of two competing modes since the amplitude variables used in the equations are the result of a somewhat arbitrary selection of basis states for the vector field. Only when the couplings and anisotropies lead to the privileged distinction of two eigenstates does it make sense to refer to those states as modes. Otherwise one has the added artificial confusion that the circularly polarized ''modes'' (which we prefer to call components of the vector field amplitude) find ways to phase lock to form linearly polarized or elliptically polarized ''states,'' an unfortunately and excessively complicated language for the dynamics and the steady states of the vector field. Nevertheless, mesurements of the intensity fluctuations of either linearly polarized or circularly polarized components of the total field can be accomplished by well-defined experimental techniques.

The remainder of this paper is organized as follows. In Sec. II we introduce the model on which our calculations are based together with the basic variables and relevant correlation functions used for characterizing the statistical properties of the intensity and polarization fluctuations. In particular we introduce two different measures of the intensity linewidth that only coincide when a single time scale is relevant in the problem. In Sec. III we analyze more exactly the condition when the total output power of the laser can be assumed to be constant. Within this approximation a potential description of the motion of the polarization under the action of the noise is possible. This permits us to identify different dynamical regimes. Also within this approximation we derive analytically, *in a nonperturbative fashion*, results for intensity correlations and intensity linewidths. These general results are discussed separately for the weak- and strong-coupling cases in Secs. IV and V. For the strong-coupling case we further introduce the concept of a restricted ensemble to describe polarization fluctuations in finite observation times and our results are compared with the behavior found in computer simulations of the complete equations. Section VI gives a unified view of our results for weak and strong coupling in terms of the basic parameter of the theory that measures the relative strength of the saturation asymmetries and noise intensity. PS behavior is characterized by a single time scale associated with polarization diffusion. A single dominant time scale associated with SM behavior is also reached, through intermediate crossover regions, for strong material cross-saturation preferences for linearly or circularly polarized emission. While most of our mathematical formulation is developed for the case of an isotropic cavity, in Sec. VII we address the effects of cavity anisotropies on our previous results. A summary of our results and some concluding remarks are given in Sec. VIII. Appendixes A and B contain some details of the calculations.

II. MODEL, VARIABLES, AND CORRELATION FUNCTIONS

We consider the following third-order Lamb model for the evolution of the two circularly polarized components $E_{\pm}$ of the electric field amplitude of a laser operating on a single spatial mode [2,3]

$$\dot{E}_{\pm}=[\alpha-\beta(|E_{\pm}|^2+\gamma|E_{\mp}|^2]E_{\pm}+\sqrt{\epsilon}\Sigma_{\pm}. \tag{1}$$

The additive noise terms $\Sigma_{\pm}$ account for spontaneous emission in the cavity and are assumed to be uncorrelated Gaussian white-noise sources

$$\langle\Sigma_p^*(t)\Sigma_q(t')\rangle=2\delta_{p,q}\delta(t-t'), \tag{2}$$

where $p,q=\pm$. The two circularly polarized components of the vector field amplitude are related to the linearly polarized components $E_{x,y}$ by

$$E_{\pm}=\frac{E_x\pm iE_y}{\sqrt{2}}. \tag{3}$$

Intensities are defined by the moduli of these amplitudes $I_{\pm}=|E_{\pm}|^2$ and $I_{x,y}=|E_{x,y}|^2$, while the total intensity is given by $I=I_++I_-=I_x+I_y$. In Eq. (1) the parameter α is proportional to the difference between the pump rate and a threshold level, i.e., it is positive above threshold. The nonlinear term takes into account saturation of gain in the framework of third-order Lamb theory (parameter β). For simplicity in the present study we take both α and β to be real, so that we consider a laser with the cavity perfectly tuned to the atomic resonance.

Polarization preference arising from saturation of the material lasing transition is introduced in the nonlinear gain saturation terms by the γ parameter [3,35,36]. For transitions involving angular momenta $j\rightarrow j$ $(j>1)$ there is *strong coupling* $(\gamma>1)$, while with a lasing transition $j=1/2\rightarrow j=1/2$ or $j\rightarrow j+1$ with $j>0$ there is *weak coupling* $(\gamma<1)$. We will use the reparametrization $\gamma=1-\delta$ so that strong coupling is given by $\delta<0$ and weak coupling by $\delta>0$. For $j=1\rightarrow j=1$ and for $j=1\rightarrow j=0$ there is neutral coupling $(\delta=0)$ except for dissipative processes, which can lead either to $\delta>0$ of $\delta<0$ [2,21,46].

From a *deterministic* point of view $(\epsilon=0)$, neutral coupling $(\delta=0)$ gives a situation that is invariant under changes

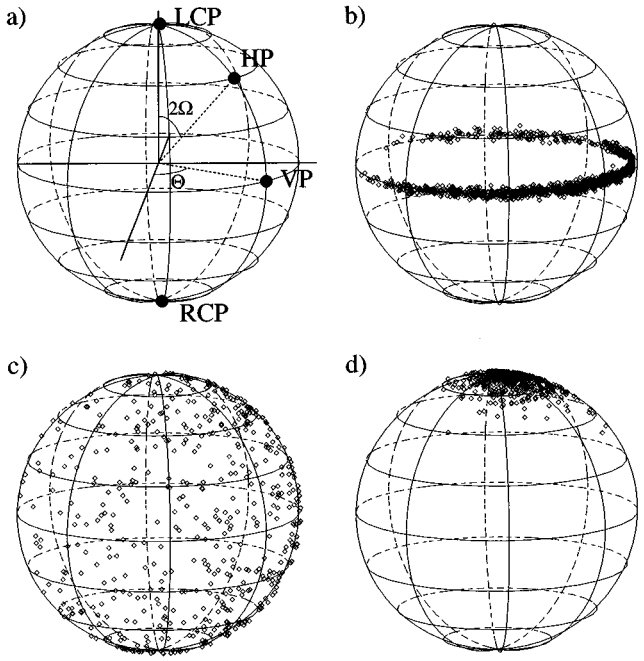

FIG. 1. (a) Poincaré sphere. (b)–(d) Evolution of the polarization on the Poincaré sphere with points indicating instantaneous positions at regular intervals of time: (b) weak coupling $\delta>0$, (c) intermediate coupling (symmetric case) $\delta\simeq 0$, and (d) strong coupling $\delta>0$.

in the polarization state. Weak coupling between the two circular amplitudes $\delta>0$ leads to linearly polarized emission (which can be viewed as coexistence of the circularly polarized modes with $I_+=I_-$) with an arbitrary vector orientation. Strong coupling $\delta<0$ leads to a preference for circularly polarized emission with two possible equivalent states, either $I_+\neq 0$ or $I_-=0$ or vice versa. We will discuss in this paper how the effect of noise modifies this picture.

Equation (1) is similar to the semiclassical Langevin equations considered, for example, in Ref. [27], where cavity phase anisotropy and linear gain differences between the two different linearly polarized components of the vector field were included. Cavity anisotropies introduce a mechanism that competes with the one of nonlinear gain saturation in the process of selection of a polarization state. We consider first a perfectly isotropic cavity and defer the discussion of the effects of cavity anisotropies to Sec. VII.

To introduce relevant variables for our analysis we write Eq. (1) in terms of phases and amplitudes defined as

$$E_\pm(t)=R_\pm(t)\exp[i\phi_\pm(t)]. \tag{4}$$

Using Ito stochastic calculus [47], we get for the amplitudes

$$\dot R_\pm=\{\alpha-\beta[R_\pm^2+(1-\delta)R_\mp^2]\}R_\pm+\frac{\epsilon}{2R_\pm}+\sqrt{\epsilon}\xi_\pm \tag{5}$$

and for the phases

$$\dot\phi_\pm=\sqrt{\epsilon}\frac{\eta_\mp}{R_\pm}, \tag{6}$$

where $\eta_\pm$ and $\xi_\pm$ are uncorrelated and real white-noise sources.

It is natural to rewrite the amplitude equations by introducing ''polar'' coordinates, with the angle

$$\Omega=\tan^{-1}(R_-/R+) \tag{7}$$

and the radius $R=\sqrt{I}$. These variables and the phases $\phi_\pm$ are related to the polarization ellipse: The angle Ω is related to the ellipticity of the polarization ellipse (χ) by $\Omega=\chi+\pi/4$ and $\theta/2=(\phi_+-\phi_-)/2$ gives the orientation of the azimuth of the polarization ellipse. In the representation on the Poincaré sphere [see Fig. 1(a)], the radius is R, the latitude angle is 2Ω, and the longitude angle is θ.

For R and Ω the following Langevin equations hold:

$$\dot R=\left\{\alpha-\beta\left[\left(1-\frac{\delta}{2}\sin^2(2\Omega)\right)R^2\right]\right\}R+\frac{3\epsilon}{2R}+\sqrt{\epsilon}\xi_R, \tag{8}$$

$$\dot\Omega=\frac{\epsilon}{R^2}\cot(2\Omega)+\frac{\beta\delta R^2}{4}\sin(4\Omega)+\sqrt{\epsilon}\frac{\xi_\Omega}{R}, \tag{9}$$

where the noise terms have correlations given by

$$\langle\xi_p(t)\xi_q(t')\rangle=\delta_{p,q}\delta(t-t') \tag{10}$$

and $p,q=R,\Omega$. Equations for the phases $\phi_\pm$ are easily rewritten in terms of these new variables by substituting $R\cos\Omega$ and $R\sin\Omega$ for $R_\pm$, respectively, in Eq. (6).

If the total intensity of the field remains constant, the polarization state can be mapped onto the surface of a Poincaré sphere. The qualitative behavior of noise-driven polarization as found in numerical integration of Eq. (1) is shown in Figs. 1(b)–1(d). For weak coupling ($\delta>0$) there is diffusion around the equator [Fig. 1(b)]. This means that the polarization observed over short time intervals is almost always linear, but the orientation diffuses under the action of the noise as recently observed experimentally [30,32]. For neutral coupling [Fig. 1(c)] we have a situation in which there is diffusion over the whole sphere. In contrast, for strong coupling ($\delta<0$) the solution is confined around the poles [Fig. 1(d)], which means an almost circularly polarized state with weakly fluctuating ellipticity.

We characterize the dynamical features of the polarization fluctuations by looking at different correlation functions of the intensity fluctuations. The correlation function for the intensity fluctuations of one of the circularly polarized components (CCF) is

$$C_+(t)=\langle I_+(t)I_+(0)\rangle-\langle I_+\rangle^2 \tag{11}$$

and the correlation function for the intensity fluctuations of one of the linearly polarized components (LCF) is

$$C_x(t)=\langle I_x(t)I_x(0)\rangle-\langle I_x\rangle^2. \tag{12}$$

When the total intensity has negligible fluctuations, the CCF gives information about correlations of the latitude angle. In the case shown in Fig. 1(b), in which the motion is practically confined to the equator of the Poincaré sphere, the LCF gives information about diffusion along this circle. In the following, unless explicitly stated otherwise, we will always

refer to the correlations of the fluctuations of the intensities of the circularly polarized components.

To calculate the correlation times and the associated linewidths we use the representation of a general correlation function of fluctuations around a stationary state

$$C_+(t)=\sum_k R_k \exp(-\lambda_k t), \tag{13}$$

where $\lambda_k>0$. We will consider ''moments'' μ_n of the inverse correlation times λ_k,

$$\mu_n=\frac{\sum_k R_k \lambda_k^n}{\sum_k R_k}, \tag{14}$$

which give information about characteristic times (and therefore linewidths) associated with the correlation function. Generally speaking, the first moment gives a measure of the *average* linewidth and coincides with the linewidth observed in an experiment only when there is a single dominant time scale involved. In other words, the observed spectrum is purely Lorentzian only in this case.

The moments μ_n can be rewritten in terms of the derivatives of the correlation function evaluated at zero time difference [45]

$$\mu_n=(-1)^n \lim_{t\to 0^+} \frac{1}{C(0)} \frac{d^n C_+(t)}{dt^n}. \tag{15}$$

Using this relation, it is possible to calculate dynamical properties such as correlation times as averages over stationary distributions of the intensity. For small fluctuations around a single stationay state, there is a single time scale and consequently the variance of the correlation times is zero. However, in the case of bistability, several time scales are involved in the decay of the correlation function, corresponding to different characteristic time scales for the evolution of a trajectory on the Poincaré sphere. For example, for strong coupling there is bistability between the right and left circularly polarized solutions. We will show in Sec. III that this can be described in terms of a potential with minima associated with the two circularly polarized states. There are then time scales for hopping between the potential minima that depend exponentially on the height of the potential barrier between the minima and there is also a much shorter time scale associated with fluctuations around either of the minima. In this case we expect the variance of the inverse time scale to be large.

Instead of directly comparing the moments μ_n we can consider another measure of the maximum time scale. The harmonic mean provides an estimate of the maximum within a distribution of possible linewidths,

$$\mu_{eff}^{-1}=\frac{\sum_k R_k/\lambda_k}{\sum_k R_k}. \tag{16}$$

This quantity is simply related to the integral of the correlation function

$$\mu_{eff}^{-1}=\frac{1}{C(0)}\int_0^\infty dt\ C_+(t). \tag{17}$$

The quantity μ_{eff} is interpreted as the ''effective linewidth'' for the intensity fluctuation spectra taken *for very long observation times*.

In the following sections we will use both μ_n and μ_{eff} to characterize the intensity fluctuation linewidths in different dynamical regimes. The comparison of these two quantities will enable us to identify regimes in which more than one time scale is relevant.

III. APPROXIMATION OF CONSTANT TOTAL INTENSITY

Polarization partition noise refers to the usual situation in which the total laser intensity remains essentially constant while the intensity associated with each of the two orthogonally polarized components fluctuates in time. We address this problem by first assuming that the total laser intensity I remains strictly constant in time. This will allow us to study the motion of a single independent degree of freedom: the angle Ω defined in Eq. (7). As a consequence of this approximation both measures of the correlation times discussed above can be evaluated analytically.

In this approximation Eq. (9) for Ω can be rewritten as an overdamped motion of a particle in a potential V,

$$\dot{\Omega}=-\frac{\epsilon}{I}\left(\frac{dV}{d\Omega}\right)+\sqrt{\frac{\epsilon}{I}}\xi, \tag{18}$$

where I is the steady-state total intensity and the new real white-noise source ξ has unit variance. The potential V is the sum of two terms $V=V_s+V_{as}$,

$$V_s(\Omega)=-\frac{1}{2}\ln[\sin(2\Omega)],$$

$$V_{as}(\Omega)=\frac{a}{16}\cos(4\Omega), \tag{19}$$

of which only V_{as} depends on the strength of the cross saturation through the parameter a defined as

$$a=\frac{\beta\delta I^2}{\epsilon}. \tag{20}$$

This is the relevant parameter of the theory. It is worth noting that the motion of Ω is decoupled from that of the phases $\theta_\pm$ and so it is also decoupled from the motion of the orientation θ of the polarization ellipse. However, from Eq. (6) we see that the phases are not decoupled from the fluctuations of either the intensity or the polarization orientation. V_{as} gives a term explicitly independent of the noise in the equation for Ω, while V_s is proportional to the noise strength. The latter originates in the change of variables used for our stochastic description.

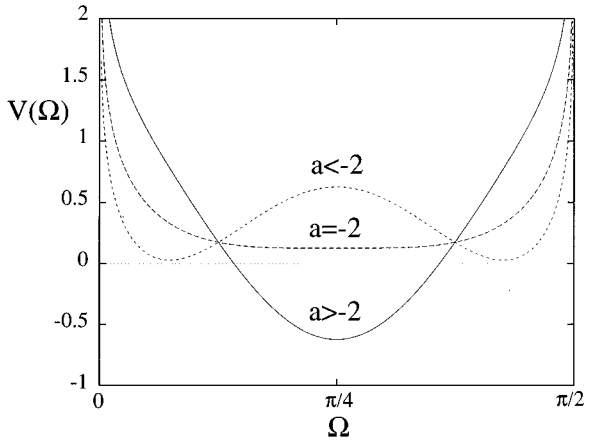

FIG. 2. Sketch of the potential $V(\Omega)$ defined in Eqs. (19).

The contribution to the potential V_{as} from the cross-saturation parameter changes the shape of the total potential V from a single well ($a>-2$) to a double well ($a<-2$) (see Fig. 2). This change reflects a competition between fluctuations and the polarization state preference (given by the strength of the cross-saturation parameter), which will be discussed separately for the cases of weak and strong coupling.

(a) Weak coupling ($\delta>0$). In this case there is a preference for linearly polarized emission as described by the minimum of the potential at $\Omega=\pi/4$. We obtain a linearly polarized state in which $I_+=I_-$. From Eq. (18), neglecting the noise terms, we obtain the equilibrium total intensity $I=I_0/(1-\delta/2)$, where $I_0=\alpha/\beta$ [48]. In terms of the representation of the field on the Poincaré sphere, the equilibrium states lie on the equator (see Fig. 1). For stochastic dynamical evolution we expect to find one of three situations: (i) fluctuation-dominated dynamics among different latitudes of the Poincaré sphere, (ii) a situation in which the force associated with V_s and the force associated with the polarization state preference given by V_{as} are of the same order, and (iii) a situation in which the polarization state preference from the cross-saturation parameter dominates and the motion of the variable Ω is strictly confined near states of linear polarization $\Omega=\pi/4$. In the first case the free fluctuations of the field are expected to result in a large correlation time for the intensity in one polarization state. In the third case the variable Ω suffers many scatterings from the high walls of the potential that rapidly decorrelate its motion. The second case corresponds to a crossover dynamical regime.

(b) Strong coupling ($\delta<0$). In the absence of fluctuations this leads to a preference for circularly polarized emission. However, in the presence of fluctuations we have to distinguish three qualitatively different regimes. For $a>-2$ the potential has a single well, which means that the angle Ω diffuses over the different latitudes of the Poincaré sphere in a manner closely similar to the behavior in the PS case. For $a<-2$ there is a potential barrier of height approximately equal to $|a|/4$ that separates the two stable equilibrium states. These states approach the values $\Omega=0$, i.e., circularly polarized $-$, and $\Omega=\pi/2$, i.e., circularly polarized $+$, for large values of $|a|$. Again from Eq. (8) we recover the result that the total intensity $I=I_0$. Also in this case we expect a crossover in the dynamical behavior of the system once the polarization preference from the cross-saturation parameter becomes relevant (through an increase of the barrier height), making the steady states almost purely circularly polarized states.

Two subcases are possible: (i) polarization hopping (PH), when one views the system long enough to see polarization hoppings between the $+$ and $-$ states, and (ii) trapping around a circularly polarized state, if the system remains around a particular circularly polarized state for a time longer than the observation time.

Therefore, in both cases (a) and (b) we expect a crossover in the dynamical quantities when $|a|$ is of order unity, i.e., when δ is of the order of the noise strength. The condition of criticality $a=-2$ (the absence of a quadratic term in the potential V) does not coincide with the marginal coupling in which $a=0$. This can be understood by looking at the stationary distribution function of the intensity.

In terms of the potential, the stationary distribution function of the variable Ω is

$$P(\Omega)\propto\exp-2[V_s(\Omega)+V_{as}(\Omega)]. \tag{21}$$

The distribution for one of the intensities is readily obtained using the definition of Eq. (7) together with Eqs. (19),

$$P(I_+)\propto\exp\left[a\frac{I_+}{I}\left(1-\frac{I_+}{I}\right)\right]. \tag{22}$$

When $a=0$ the equilibrium distribution function of the intensity in a definite polarization state is flat, indicating that there will be rapid diffusion over the entire Poincaré sphere. In this case $P(\Omega)$ gives the appropriate geometrical factor $\sin(2\Omega)$ needed to have a flat intensity distribution as expected for $a=0$. This distribution of Ω also can be obtained by considering a free particle diffusing on the surface of a sphere. In principle, the descriptions of equilibrium properties in terms of the *angle* Ω as in Eq. (21) or in terms of the intensity as in Eq. (22) are equivalent, but in the discussion of the properties of the intensity process we will use the angular variable that is driven by purely additive noise. Because of this property, the inverse correlation time μ_{eff} can be evaluated easily. The correlation function $C_+(t)$ defined in Eq. (11) as a function of variable Ω is

$$C_+(t)=I^2[\langle\cos^2\Omega(t)\cos^2\Omega(0)\rangle-1/4]. \tag{23}$$

With the help of Eq. (15) we calculate correlation times as averages over equilibrium distributions of the variable Ω.

We make use of a general result that holds for functions of stochastic processes reported in Appendix B. This enables us to calculate, in principle, all moments of the characteristic inverse time using Eq. (B6) together with Eq. (15). To obtain μ_n it is useful to normalize Eq. (18), redefining a time scale by $\tau=\epsilon/I$ so that the normalized linewidth Γ_n is defined through

$$\mu_n=\Gamma_n\epsilon/I. \tag{24}$$

If we restrict our consideration to the case $n=1$, we can use Eq. (B8) together with Eq. (15) to get, in terms of the process Ω,

TABLE I. Asymptotic results for the linewidths.

a	Γ_1	Γ_{eff}	Γ_{1+}
$\ll -1$	$\frac{8}{\lvert a\rvert}$	$\frac{(\lvert a\rvert)^{3/2}}{\sqrt{\pi}}\exp(-\lvert a\rvert/4)$	$2\lvert a\rvert$
0	4	4	
$\gg 1$	$a-2$	$a-2$	

$$\Gamma_1 = 2\frac{\langle \sin^2(\Omega)\cos^2(\Omega)\rangle}{\langle \cos^4(\Omega)\rangle - \langle \cos^2(\Omega)\rangle}. \tag{25}$$

The analytical result valid for both signs of the saturation asymmetry parameter δ (linear or circular polarization preference) is

$$\Gamma_1 = \frac{(a-2)A_0(a) + \exp(-a/4)}{A_0(a) - \exp(-a/4)}, \tag{26}$$

where A_0 is given in terms of the error function (of complex argument if $a<0$)

$$A_0(a) = \sqrt{\frac{\pi}{a}}\,\mathrm{erf}(\sqrt{a/4}). \tag{27}$$

Using the constant intensity approximation, it is also possible to give an analytical formula for Γ_{eff} obtained from μ_{eff} [Eq. (16)] through the rescaling of Eq. (24). Following the method in [49], it is possible to evaluate the effective linewidth as

$$\Gamma_{eff}^{-1} = \frac{1}{C(0)}\int_0^{\pi/2} d\Omega\ P(\Omega)^{-1}, f^2(\Omega), \tag{28}$$

where

$$f(\Omega) = -I\int_0^{\Omega} d\Omega' P(\Omega')[\cos^2(\Omega') - \langle \cos^2(\Omega)\rangle]. \tag{29}$$

To obtain this relation we have taken advantage of the fact that the Langevin equation (18) involves only one degree of freedom with a purely additive noise. The average linewidth Γ_1 could be evaluated by relaxing the constant intensity approximation, as done, for example, in Ref. [45], but to get the effective linewidth Γ_{eff} by analytical calculations as far as possible the approximation of constant I is crucial. Moreover, given the probability distribution function (21), we can carry out the integral of Eq. (29) analytically, obtaining

$$\Gamma_{eff}^{-1} = \frac{1}{2a^2 A_2}\int_0^1 dx \frac{\sinh^2[ax(1-x)/2]}{x(1-x)}, \tag{30}$$

where A_2 is given in Eq. (A3).

Equations (26) and (30) give explicit values for the linewidths defined in general in Sec. II. Some useful values obtained using the asymptotic expansion of the error function appearing in Eq. (27) are shown in Table I. Separate discussions of the weak- and strong-coupling cases of our results for the linewidths are given in Secs. IV and V. We now briefly discuss the range of validity of the constant intensity approximation. Consider the most restrictive case of having ''small'' fluctuations around one particular steady state. This occurs for $|a|\gg 1$ when the point representing the polarization on the Poincaré sphere is confined around the poles ($a \ll -1$) or equator ($a\gg 1$). In Appendix A we obtain the fluctuation of the partial intensity around a preferred circularly polarized state [Eq. (A13)] and around a linearly polarized state [Eq. (A6)]. By comparing these results with the total intensity fluctuations we have an estimate of the validity of the approximation.

To evaluate the total intensity fluctuations let us consider the case $|\delta|\ll 1$. Then the term dependent on the saturation asymmetry ($\delta\neq 0$) can be neglected and, provided the noise is not large, i.e., supposing the laser is well above threshold, we can neglect the term proportional to ϵ/R in Eq. (9), thereby obtaining an equation similar to that of a SM laser. In this case the fluctuations of the total intensity are $\langle \Delta I^2\rangle = \epsilon I_0/\alpha$. We thus neglect the total intensity fluctuations with respect to the average intensity in the limit $I_0 \gg \epsilon/\alpha$, provided $\delta \ll 1$ [50]. The ratio between the partial and the total intensity fluctutions is readily obtained by taking into account Eqs. (A6) and (A13),

$$\langle \Delta I^2\rangle / \langle \Delta I_+^2\rangle = 2\delta \quad \text{for} \quad a\gg 1, \tag{31}$$

$$\langle \Delta I^2\rangle / \langle \Delta I_+^2\rangle_+ = a\delta \quad \text{for} \quad a\ll -1, \tag{32}$$

where the subscript $+$ in Eq. (32) indicates an average restricted to states around one of the two equivalent circularly polarized states (see Sec. V). The condition for the validity of our approximation is much more restrictive in the case of cross-saturation preference for circularly polarized emission. This can be understood from the potential picture. In Fig. 2 we see that the shape of the potential with strong coupling is such that the motion of Ω is more strictly confined to one definite angle (due to infinitely high barriers at $\Omega = 0, \pi/2$) than in the case of weak coupling. However, it is sufficient to have a small value of the cross-saturation asymmetry δ for this approximation to be valid.

IV. WEAK COUPLING

Results for μ_1 and μ_{eff} obtained, respectively, from Eqs. (26) and (30) for the weak-coupling case ($\delta>0$) are shown in Fig. 3. We observe a crossover from PS-like behavior in which the linewidth decreases with total output intensity to SM-like behavior in which it increases. This crossover occurs at a pump value that decreases as the cross-saturation asymmetry parameter δ increases. Our calculations are based on the assumption that the noise amplitude ϵ is independent of the output power, a resonable assumption if the clamping of the population inversion clamps the population in the upper level, which is the case for most laser media that have a much more rapid decay rate for the lower level. The crossover also can be understood qualitatively from the potential picture. At a fixed value of saturation asymmetry parameter δ, when the laser intensity increases, the parameter a also increases. As the value of a increases, the system passes from an almost flat potential in which the motion of the intensity is similar to that in a PS laser ($\delta=0$) to a very deep single-well potential (see Fig. 2). In this last situation the

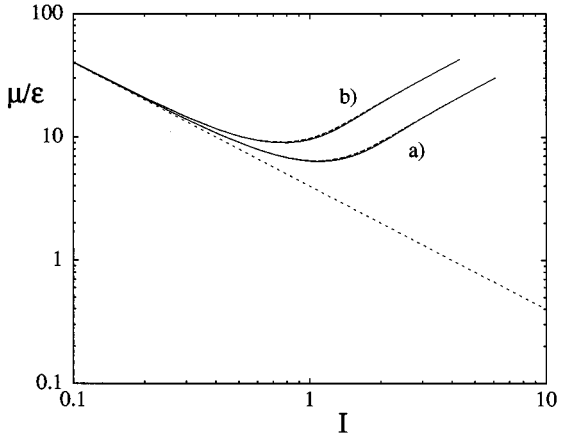

FIG. 3. Linewidth μ as a function of the total output intensity I scaled to the noise strength ϵ in the case of weak cross-saturation coupling. The units of the scaled linewidth are the inverse of intensity units. The parameter values are (a) $\delta=5\epsilon$ and (b) $\delta=10\epsilon$. The continuous lines give the effective linewidth μ_{eff}, the long-dashed lines give the average linewidth μ_1, which practically coincides with μ_{eff} except around $I\simeq 2$, and the short-dashed line gives the PS case ($\delta=0$) in which the two quantities coincide exactly.

intensity of a single circularly polarized component has small fluctuations, measured by $C_+(t)$, similar to those of a SM laser.

In terms of the same potential picture it is also possible to understand the small deviations between μ_{eff} and μ_1 observed for intermediate values of the intensity. To explain this let us consider the two opposite cases of the PS laser and the SM laser. For the PS case, as shown in Ref. [25], the system is subject to diffusion on a four-dimensional sphere. In the SM case the intensity is subject to small fluctuations around a single equilibrium state. In the case of purely diffusive motion, as well as for a linear process, we expect only one time scale to be relevant, i.e., the diffusion constant or the amplitude of the restoring force that leads to the equilibium. For the PS case this argument is in agreement with the quantitative results of Ref. [25], in which by taking the same approximation of a nonfluctuating total intensity only one time scale was found. Thus when the system behaves like a PS laser or when it behaves like SM laser we should observe a single Lorentzian spectrum. As a consequence, the deviations from a Lorentzian spectrum that imply $\mu_{eff}\neq\mu_1$ mark the crossover region.

The output intensity at the crossover point can be estimated by equating the small intensity linewidth, which is well approximated by the symmetric $a=0$ result, and the large positive a results given in Table I, obtaining $a_{cross}=6$ and

$$I^2_{cross}\simeq 6\epsilon/\beta\delta. \tag{33}$$

The pump parameter at the crossover is

$$\alpha^2_{cross}\simeq 6\epsilon\beta/\delta. \tag{34}$$

We have implicitly assumed small positive saturation values for δ, i.e., slightly in the weak-coupling situation, such that $I\simeq I_0=\alpha/\beta$. When δ is of the order of the noise strength ϵ, we have an intensity and pump parameter of order one at the crossover, that is, far above the lasing threshold.

Below I^2_{cross} [Eq. (33)] the statistical properties of the intensity fluctuations of the polarization asymmetric laser are similar to those of a PS laser, while above that value they are similar to those of the SM laser because the parameter a is large enough for the laser to work very close to pure linear polarization.

Up to this point we have discussed stochastic properties of the angle Ω, which is related to the ellipticity of the polarization state. Increasing the parameter a when the coupling is weak leads to states of more and more stable linear polarization. The motion of the state of polarization on the Poincaré sphere is confined to the neighborhood of the equator [see Fig. 1(b)]. In the absence of cavity anisotropies we expect diffusion along the equator [30], corresponding to diffusive motion of the phases $\phi_\pm$ in Eq. (6). We recall that the orientation of the polarization ellipse's main axis is $\theta=\Phi_+-\Phi_-$. We can describe this diffusion process by the linewidth of the correlation function of the intensity fluctuations of the linearly polarized components defined in Eq. (12). The intensity of the x-polarized component of the laser emission can be written as

$$I_x=I/2+R_+R_-\cos(\phi_+-\phi_-), \tag{35}$$

so that the correlation properties of the phase difference can be addressed by the study of C_x. For a strong linear polarization preference, i.e., when $a\gg 1$, this relation is very simple. In this case, neglecting also the fluctuations of the circular polarized amplitudes $R_\pm$, the time dependence of the correlation function C_x is entirely due to the diffusion of the phases ϕ_+ and ϕ_-. One has

$$C_x(t)=\text{const}\times\exp(-\mu_x t), \tag{36}$$

where $\mu_x=\langle\phi_+(t)\rangle/t=$ is the diffusion coefficient of the phase. Via Eq. (6) we get

$$\mu_x=\epsilon/I, \tag{37}$$

i.e., the normalized linewidth is $\Gamma_x=1$. A duality exists between the intensities of the $\pm$ components of the vector field and the intensities of the x,y components: When the first has short time correlations due to confinement, the second has a very long correlation time due to diffusion. A similar phenomenon occurs in a SM laser when one compares the intensity fluctuation spectrum with the field spectrum. In this case the loss of phase coherence due to phase diffusion is evident in the field-field correlation function rather than in the intensity correlation function.

V. STRONG COUPLING

Results for the linewidths μ_1 and μ_{eff} for strong coupling ($\delta>0$) are shown in Fig. 4. For low intensities the linewidth initially behaves as in the PS laser. Then the two measures of the linewidth diverge both from the PS result and from each other. This is understood in terms of the potential picture of the motion of the polarized intensity discussed in Sec. III. When the output intensity increases, the modulus of the parameter a increases and the potential develops a barrier. The linewidth is similar to that of the PS laser, when this barrier

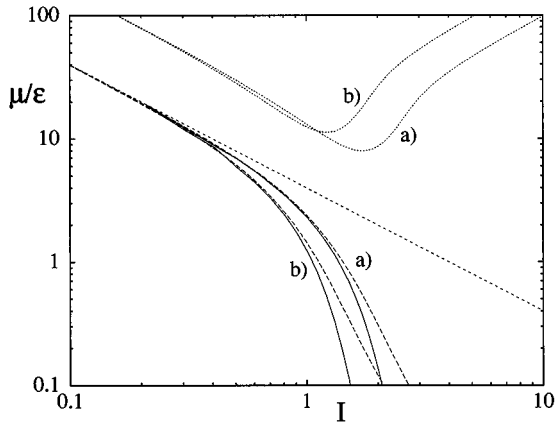

FIG. 4. Same quantities as in Fig. 3 in the case of strong coupling. The parameter values are (a) $\delta=-5\epsilon$ and (b) $\delta=-10\epsilon$. The continuous lines give μ_{eff}, the long-dashed lines give μ_1, the short-dashed line gives the PS case ($\delta=0$), and the dotted upper lines give the results of the restricted ensemble calculation μ_{1+}.

is very low or nonexistent ($a>-2$). When the barrier height increases, the system is trapped near one of the circularly polarized states, but it hops from time to time to the other state. As a consequence, several time scales are involved in the correlation function. Short time scales are associated with fluctuations near one of the two equivalent minima and long time scales are associated with the hopping motion. The presence of the first time scale is responsible for the fact that the average value of the linewidth μ_1 is always greater than its effective value μ_{eff}. In this regime the spectrum is non-Lorentzian.

When the output intensity increases, there is an exponential decrease of the effective linewidth, which is given by the asymptotic expansion result shown in Table I. The asymptotic exponential behavior is due to barrier hopping and could also be recovered by using a simple Kramer argument. Due to the exponential decrease of the linewidth there is an ''observation limit.'' Beyond this limit, in a measurement of practical duration one would typically find only one polarization state as an apparently stable output with small fluctuations.

To characterize the fluctuations around each minimum of the potential in this case of preference for circularly polarized emission, we must restrict the observation time to a time scale much less than the time needed to hop from one polarization state to the other. The barrier between the two minima is approximately of height $|a|/4$ for large $|a|$. This causes the time of hopping from one minimum to the other to increase exponentially as the strength of the cross-saturation parameter increases. Using a simple Kramer argument, we find for large $|a|$

$$T_{hop}=T_0\exp(|a|/4), \tag{38}$$

where T_0 is a characteristic time that depends on the dynamics around the minima and maxima of the potential [49] and T_{hop} is the the mean first-passage time over the barrier. If we restrict the time of observation to a time much smaller than this mean hopping time, we will not see any polarization hops between the $+$ and $-$ states. For large $|a|$, this time is large enough to give rise to a quasiequilibrium distribution function between hops.

An estimate of this quasiequilibrium distribution function can be obtained by introducing a *restricted ensemble* of realizations of I_+ defined as realizations that fulfill the condition $I_+>I/2$. This condition is equivalent to selecting realizations of the process that stay around the $+$ circularly polarized state. We define the average over such a restricted ensemble of a generic function of I_+ as

$$\langle f(I_+)\rangle_+=\int_{I/2}^{I} f(I_+)P(I_+)dI_+, \tag{39}$$

where $P(I_+)$ is given by Eq. (22) normalized to one in the interval $[I/2,I]$. Moments of the partial intensities evaluated in this restricted ensemble are given in Appendix A.

Dynamical properties over time scales in which the system is trapped around one definite polarization state are described by considering correlations of the process Ω assuming a single restricted ensemble of realizations. It is important to stress again that if the state of the system fluctuates around the circularly polarized states, i.e., if we consider realizations belonging to a restricted ensemble, then we expect only one time scale to be involved in the correlation function of the intensity fluctuations. In this case the calculation of Γ_1 and Γ_{eff} in the restricted ensemble have to give the same result. For the sake of simplicity we calculate only Γ_1 in a restricted ensemble. By performing the average of Eq. (25) and taking into account the definition of Eq. (39) and the results of Appendix A, we have

$$\Gamma_{1+}=\frac{(a-2)A_0(a)+\exp(-a/4)}{A_0(a)-\exp(-a/4)-[1-\exp(-a/4)]^2/aA_0(a)^2}. \tag{40}$$

The asymptotic value of Γ_{1+} is also shown in Table I. Comparing the results in Table I, we see that the properties of the restricted ensemble for very strong cross saturation are similar to those of a SM laser, i.e., the linewidth grows as I^2 for large output power. Results of calculations for the restricted ensemble are shown in Figs. 4(a) and 4(b) (upper curves). These curves represent the result of a finite time window measurement of the linewidth. By contrast, for low intensities the restricted ensemble calculations have no sense since the barrier is so low that fluctuations are able to produce several hoppings during the time of observation.

As in the case of preference for linearly polarized emission we can get an estimate of the crossover intensity from a regime similar to PS to the regime for large output power. This crossover will depend on the observation time T taken to record the spectrum. Trapping in one of the two circularly polarized states is observed if the hopping time exceeds the observation time.

For very large observation times the crossover value of the parameter a is essentially given by the exponential term in Eq. (38); in other words, the time constant T_0 can be neglected if we measure times in units of I/ϵ as in Eq. (24). A justification for this can be obtained by evaluating asymptotically T_{hop} as the inverse of Γ_{eff} and then from the asymptotic expansion given in Table I to get T_0. From this

calculation it follows that the crossover value for the parameter a is given by $|a_{cross}|=4\ln(\tau_{obs})$, where τ_{obs} is the scaled observation time $\tau_{obs}=T_{obs}\epsilon/I$. In the same approximation the intensity at the crossover immediately follows

$$I^2_{cross}=4(\epsilon/\beta|\delta|)\ln(\sqrt{\beta|\delta|\epsilon}T_{obs}). \tag{41}$$

Again by setting at the crossover $I\simeq I_0$, one gets for large observation times

$$\alpha^2_{cross}\simeq 4\frac{\epsilon\beta}{\delta}\ln(\sqrt{\beta|\delta|\epsilon}T_{obs}). \tag{42}$$

To study how this crossover occurs in a realization of the stochastic intensity process we have numerically integrated Eq. (1). We have varied the nonlinear saturation coefficient β to vary the total output intensity. The cross-saturation parameter has been chosen to be slightly negative $\delta=-5\times10^{-3}$. The noise level is $\epsilon=10^{-3}$. We have used a time window $T=61\,440\alpha^{-1}$, which gives a maximum detectable linewidth of about $2\pi/T\epsilon=0.1\times10^{-3}$. The normalized spectrum of the intensity I_+ was fit with a single Lorentzian. Results are shown in Fig. 5. The same set of random numbers was used to generate the noise terms for all values of the intensities. This allows a comparison between single realizations that are defined by a particular sequence of stochastic forces $\Sigma_\pm$ in Eq. (1). The linewidth for small intensities initially fits well with the estimation μ_{eff} (continuous line in the figure). However, it departs from this theoretical infinite window limit due to the finite time window. If the time in which the process remains trapped near one minimum of the potential V is not much smaller than the time window of observation, it is likely that we will observe only a few polarization jumps. This causes the statistics of the hoppings in a single realization to be poor and gives a deviation from the infinite window limit linewidths. In other words, even a spectrum from a very long observation time window could not be fit by a simple Lorentzian since many different time scales are involved in the correlation function. Passing from $I=5$ to $I=6$, we observe an abrupt transition to a much higher value of the linewidth, which is consistent with the calculation on a restricted ensemble (dashed line in the figure).

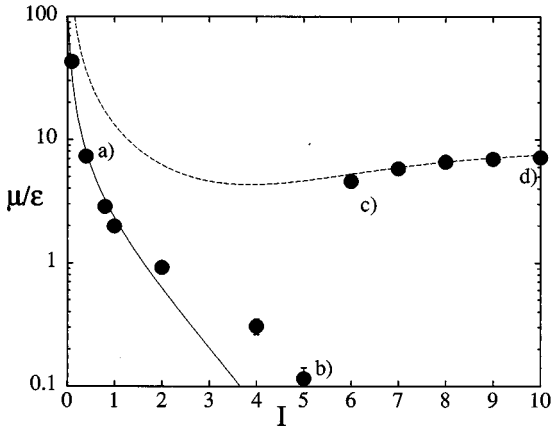

FIG. 5. Linewidth obtained by varying the parameter β to vary the total intensity ($\alpha=1$) in the strong-coupling case. Points are from simulations of Eq. (1) with parameters described in the text. The long-dashed line gives μ_{1+} and the continuous line gives μ_{eff} in units of the noise strength ϵ. a–d refer to the intensity vs time shown in Fig. 6. The finite time window induces a lower measurable limit of about 0.1ϵ.

From the intensity variation in time [see Figs. 6(a)–6(d)] we see that the transition in Fig. 5 to the linewidth value given by the restricted ensemble calculation happens when no jumps between the two circularly polarized states are found during the observation time [Fig. 6(c)]. The calculation within one restricted ensemble gives a correct approximation that works even better as the polarization fluctuations diminish with increasing pump (or, equivalently, increasing intensity). A comparison of Fig. 6(a) with Fig. 5 shows that even in the case of low intensity, in which the total intensity flucutates noticeably, our approximation of constant total intensity works quite well for the linewidth.

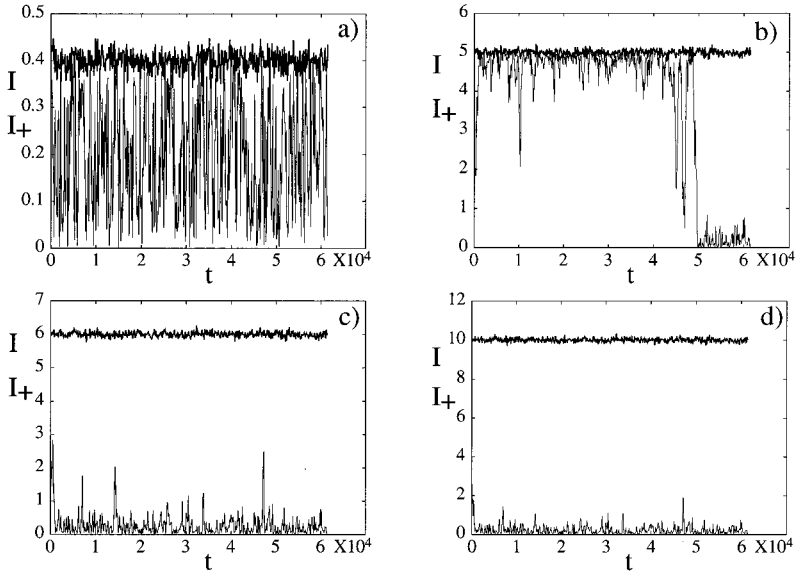

FIG. 6. Total output I (bold lines) and left circularly plus polarized I_+ (thin lines) intensities for the time window used to take the spectra shown in Fig. 5. Time is in units of the linear time scale α^{-1}. The total intensity fluctuations are always smaller than the fluctuations of the intensity of either circularly polarized component.

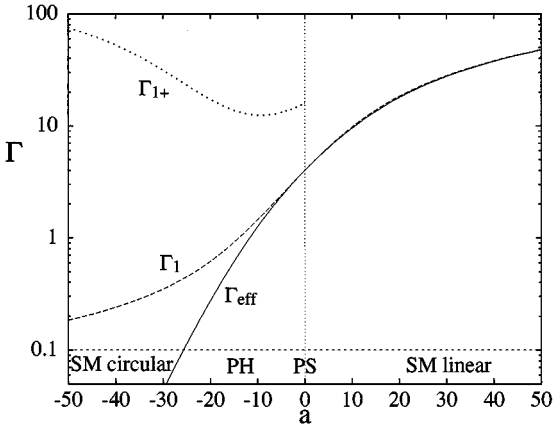

FIG. 7. Normalized linewidth as a function of the adimensional parameter a. Continuous lines give Γ_{eff}, dashed lines give Γ_1, and the dotted line gives the result of a calculation of Γ_{1+} obtained by averaging over the restricted ensemble. The lower dashed line indicates an observation time limit.

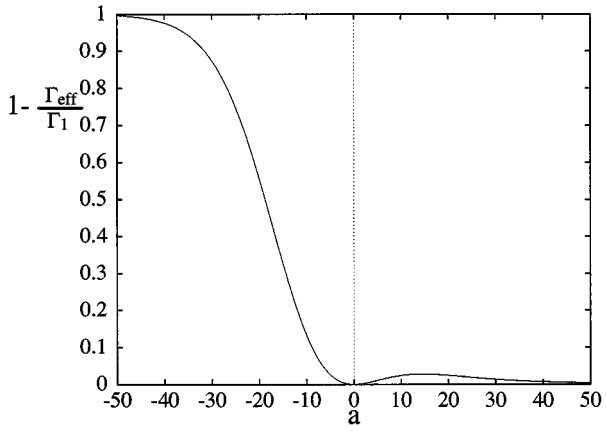

FIG. 8. Normalized ratio between the effective (Γ_{eff}) and the average (Γ_1) linewidths as a function of the asymmetry parameter a.

VI. REGIMES OF POLARIZATION FLUCTUATIONS

Figure 7 summarizes the results for the linewidth for both cases of circular polarization preference $a<0$ and linear polarization preference $a>0$ as a function of the relevant parameter of the theory a. In the marginal situation, i.e., $a=0$, the linewidth is equal to Γ_1. This is in agreement with Ref. [25], in which only one time scale in the correlation function of the fluctuations was found within the same constant intensity approximation.

Defining an observation time limit by the lower dashed line as the minimum linewidth that can be detected when taking a spectrum in a finite time, we can distinguish four regions of different behavior depending on the value of a.

(i) Polarization symmetric. This is a region near the marginal point $a=0$ (PS) in which the laser behaves as a PS laser. This region could also be defined as the region in which the intensity flucutation spectra are well fitted by a Lorentzian and as a consequence $\Gamma_1=\Gamma_{eff}$. The Lorentzian behavior of the spectra arises from the free diffusion over the whole Poincaré sphere.

(ii) Single-mode linearly polarized. Leaving the PS zone with $a>0$, Γ_1 and Γ_{eff} are slightly different. This gives an indication of a crossover regime in the a parameter space. Once a becomes large enough the two measures of the linewidth become approximately equal, indicating a single Lorentzian. This Lorentzian shape corresponds in this case to the approach to the SM-like state of linear polarization with small ellipticity (Ω) fluctuations.

(iii) Polarization hopping. Leaving the PS region with $a<0$, Γ_1 and Γ_{eff} become more and more different, indicating the increasing height of the barrier in $V(\Omega)$ with polarization hopping events in a single realization of the I_+ stochastic process. If the time window of observation is sufficiently long so that we can see many of these hoppings, the measure of the linewidth will be given by Γ_{eff}, but as we reach the observation time limit we detect motion around only one of the two circularly polarized states.

(iv) Single-mode circularly polarized. Taking a spectrum during a time window shorter than the typical trapping time we observe SM behavior of the linewidth that can be evaluated through a restricted ensemble calculation (upper dashed curve in Fig. 7).

In order to estimate the amplitude of the crossover regions we have computed the normalized difference between the two measures Γ_1 and Γ_{eff} of the linewidth. Results are shown in Fig. 8. We observe that for $a>0$ the maximum departure between average and effective linewidths occurs at a value of $a\simeq 15$ greater than the one evaluated in Sec. IV ($a\simeq 6$). For $a<0$ we notice the large departure of Γ_1 from Γ_{eff}. Around $a\simeq -6$ we have the same difference that we find as a maximum difference for $a>0$. For $a=0$ the average and effective linewidths coincide since a single time scale characterizes the diffusion process of the marginal coupling case.

In summary, there are two different regimes of crossover in a polarization asymmetric laser depending on the preferred polarization state. In both cases the laser passes from a PS-like behavior to a SM-like behavior. In the case of preference for circular polarization ($a<0$), the crossover is due to a *finite observation time* in determining the spectrum. In the opposite case in which linear polarization is preferred ($a>0$), there is crossover due to a continuous change from PS to SM. In both cases the spectrum passes through non-Lorentzian behavior. In the case of weak cross saturation (preference for linear polarization) the crossover is due to the passage from a diffusionlike behavior of the PS kind to a SM-like motion around a linearly polarized equilibrium state with equatorial diffusion. In the strong cross-saturation case (preference for circular polarization), competition between the two modes of polarization develops in a non-Lorentzian polarization hopping regime and, finally, after an observation time limit is reached, a single circular polarization is observed with a SM Lorentzian spectrum.

VII. CAVITY ANISOTROPIES

Thus far we have analyzed the polarization fluctuations of a laser in a perfectly isotropic cavity. These characteristic forms of behavior are modified, or shifted on the Poincaré sphere, by amplitude and phase anisotropies of the cavity, which can be tuned to a certain extent [32,42]. Close to the

situation of an isotropic cavity, the effect of cavity anisotropies can be described also in the context of the potential picture used in the previous sections. As a first step in this description we present here some of the main qualitative effects.

Within the general classification of cavity anisotropies of van Haeringen [51] including both linear and circular anisotropies of the losses and phases, we take a special case to gain preliminary insight and caution that a more complicated anisotropy might lead to other effects. We consider here only the special case of linear amplitude anisotropies (different losses or different linear gains for the orthogonal linearly polarized fields) and linear phase anisotropies (a frequency splitting of the linearly polarized eigenmodes such as is associated with birefringence in the medium), in the case that both of these anisotropies are diagonalized by the same pair of x and y directions. This is taken into account by adding a term to the right-hand side of Eq. (1) of the form $\rho E_{\mp}$, with ρ being a complex constant $\rho=\rho_1+i\rho_2$. The effect of these terms is more explicit in the equations for the linearly polarized components E_x and E_y of the vector field amplitude. The real part of ρ gives the different loss rates for the linearly polarized fields, while the imaginary part of ρ splits the optical frequencies of the linearly polarized steady-state solutions.

The introduction of anisotropies described by ρ modifies the equation for the total intensity R through terms that can be neglected for $|\rho|\ll\alpha$. The equation for the ellipticity becomes

$$\dot{\Omega}=\frac{\epsilon}{R^2}\cot(2\Omega)+\frac{\beta\delta R^2}{4}\sin(4\Omega)+\rho_2\sin(\theta)\sin(2\Omega)+\sqrt{\epsilon}\frac{\xi_\Omega}{R}. \tag{43}$$

For the phase difference $\theta=\phi_+-\phi_-$ we find

$$\dot{\theta}=-2\rho_1\sin(\theta)+\sqrt{\epsilon}\left(\frac{\eta_+}{R_+}-\frac{\eta_-}{R_-}\right). \tag{44}$$

Therefore, the amplitude anisotropy ρ_1 only affects indirectly the motion of Ω through the coupling with θ when there is also phase anisotropy present. On the other hand, the dynamics of θ is only affected by phase anisotropies ρ_2 in the stochastic part and through the coupling with R_+ and R_-. In the following we describe separately the cases of amplitude and phase anisotropies.

For amplitude anisotropy ($\rho_2=0$) the dynamics of Ω is not affected. The main effect is a deterministic ($\epsilon=0$) locking of the polarization ellipse orientation at $\theta=0$ or π depending on the sign of ρ_1. In the presence of noise the θ locking is effective only in the weak-coupling case $a\gg1$ in which both $R_\pm$ fluctuate around values much larger than the noise amplitude ϵ. This gives a selection among all linear polarization states that are degenerate for $\rho_1=0$. There are still small fluctuations around the two preferred linearly polarized states. Changing the value of ρ_1, we expect for $a\gg1$ a crossover in the fluctuations along the equator of the Poincaré sphere as measured by the LCF. The natural parameter to describe this crossover is $b_1=\rho_1 I/\epsilon$. A linearization procedure leads to the prediction of a μ_x that passes from a value inversely proportional to the total intensity (37) for $b_1\ll1$ to a value that depends only on the gain anisotropy ρ_1 for $b_1\gg1$. In the strong-coupling case, fluctuations of θ are huge since one of the two partial intensities I_+ or I_- is very small. The intensity fluctuates around the left circularly polarized (LCP) or right circularly polarized (RCP) states and hops between these states. Of course during the hopping process one could observe some transient locking to the $\theta=0$ or π states.

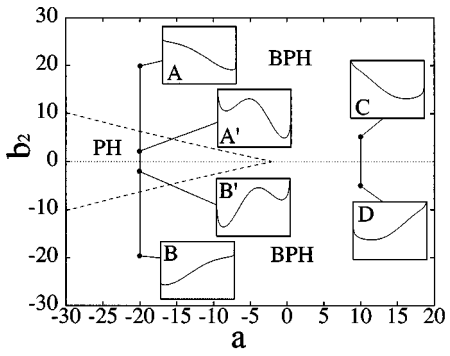

FIG. 9. Parameter space cross saturation a vs adimensional phase anisotropy b_2. In the area between the dashed line the ellipticity potential is always a double well, while outside it may be a single well depending on the value of θ. For fixed a and b_2 the polarization will run over all the states in the vertical line at constant a ranging from $-b_2$ to b_2. Three possible dynamical situations are shown: A and B, strong-coupling biased polarization hopping ($a=-20$ and $b_2=20$); A' and B', strong-coupling polarization hopping ($a=-20$ and $b_2=3$); C and D, weak-coupling biased polarization hopping (BPH) ($a=10$ and $b_2=6$). Shown in the insets are the potentials $V(\Omega)$ at the extremal points.

Let us now turn to the case of phase anisotropy ($\rho_1=0$). In this case the fluctuations of Ω are strongly correlated with fluctuations of θ. A deterministic solution of the equation for Ω is given by $\Omega=\pi/4$ and $\sin(\theta)=0$, which corresponds to linearly polarized light in the x or y direction. However, for $\rho_1=0$, θ is freely diffusing and it will only take the value $\sin(\theta)=0$ randomly. For an arbitrary value of θ the term proportional to ρ_2 in Eq. (45) produces a deterministic preference for elliptically polarized states with $\Omega\neq\pi/4$. These states are right or left elliptically polarized depending on the sign of θ and ρ_2. In the presence of noise, the potential picture that is the basis for Eq. (18) is still valid. The potential is modified by the extra term $-b_2\sin(\theta)\cos(2\Omega)/2$ and the new relevant parameter is $b_2=\rho_2 I/\epsilon$. The effect of phase anisotropy is completely masked by noise when $|b_2|\ll1$. Thus we consider only the opposite case in which phase anisotropy competes with the cross saturation measured by a. A crossover in the properties of ellipticity is expected to occur when $a\simeq b_2$. Notice that this condition, which implies $\rho_2\simeq\delta\alpha$, is still consistent with a constant total intensity, which requires $\rho_2\ll\alpha$ provided $|\delta|\ll1$. A summary of the situations that may occur in the parameter space (a,b_2) is shown in Fig. 9.

For weak coupling, if $a\gg|b_2|\gg1$ diffusion of θ is slow and we expect a motion of the mean ellipticity driven by the diffusion of the direction of the ellipse's main axes. The

situation is shown in Fig. 9 panels C and D. For a given value of b_2 the system spans the whole vertical line at a fixed value of a passing from preference for a left elliptically polarized state to preference for a right elliptically polarized state. The motion of θ induces a *biased polarization hopping* between left and right elliptically polarized states as θ crosses 0 or π during its diffusive motion.

For strong coupling, phase anisotropy gives preference for one of the two CP depending on the sign of θ and ρ_2. If $|a| \gg |b_2|$ both LCP and RCP states are (local) minima and the hopping process will be mainly determined by the presence of the barrier as in the case of panels A' and B' in Fig. 9. When b_2 increases one of the two minima disappears depending on the value of θ (panels A and B in Fig. 9). Since the remaining minimum approaches a RCP or LCP state, θ is strongly affected by noise and we expect very fast *biased polarization hopping* from LCP to RCP states and vice versa, determined essentially by the motion of θ.

The effects of saturable dispersion [an imaginary part for β in Eq. (1)] have not been included in this preliminary discussion. When this is present together with birefringence alone ($\rho_1 = 0$) and weak coupling, it privileges one of the two linearly polarized steady state solutions over the other and may destabilize one of them. This is likely to lead to biased switching between two points on the equator of the Poincaré sphere. Combinations of more general cavity anisotropies and saturable dispersion are topics of continuing investigation.

The preceding discussion gives an overview of different scenarios and regimes of polarization fluctuations when noise strength, nonlinear gain anisotropies (δ), and cavity anisotropies compete. These regimes are modified when amplitude and phase anisotropies are considered simultaneously, when other anisotropies are also considered, or when cavity detuning is taken into account. This problem requires a detailed, systematic, and more quantitative study currently being addressed.

VIII. SUMMARY AND CONCLUSIONS

We have considered statistical properties of the laser light of a nearly isotropic laser. Those have been described in terms of two measures of the linewidth of the intensity fluctuations of one of the circularly polarized components of the vector field. A comparison of those two measures identifies crossover regimes in which more than one time scale comes into play. The approximation of constant total output power allows us to obtain a number of explicit analytical results. It also results in a potential picture for the dynamics of the ellipticity on the Poincaré sphere that gives important physical insight into the laser field fluctuations. Most of our analysis refers to the fluctuations of the ellipticity, while other studies have focused on the fluctuations of the direction of linearly polarized emission [30,31]. The coupling of these two types of fluctuations due to cavity anisotropies gives rise to enhanced fluctuations as described in Sec. VII.

The competition of laser anisotropies (from gain saturation of the cavity), which tend to stabilize some particular type of polarization state, and spontaneous emission noise, which produces randomizing polarization excursions, leads to different regimes of polarization fluctuations and crossovers among them. These have been analyzed in the weak- and strong-coupling regimes in terms of a single relevant parameter that measures the relative strength of the competing mechanisms. Explicit results for the intensity fluctuation linewidth have been given in terms of this parameter. For weak coupling the crossover is from a polarization symmetric laser to linearly polarized emission. For strong coupling the crossover to circularly polarized emission is dominated by fast hopping among circularly polarized states.

ACKNOWLEDGMENTS

We acknowledge financial support from the European Union under Contracts No. CHB-CGT93-0437 (nonclassical light) and FMRX-CT96-0066 (microlasers and cavity QED).

APPENDIX A: MOMENTS OF THE PARTIAL INTENSITY

To quantitatively check the estimation of Eqs. (31) and (32) and to provide an estimation of the relative fluctuations also on the case of $|a| \simeq 1$, we calculate all moments of the intensity fluctuations in a single polarization state. When $a < 0$, this distribution of intensity is bimodal with peaks around $I_+ = 0$ and I. The moments of the intensity fluctuations $\Delta I_+ = I_+ - \langle I_+ \rangle$ can be expressed as integrals

$$\langle \Delta I_+^n \rangle = I^n \frac{A_n}{A_0}, \tag{A1}$$

where

$$A_n = \int_{-1/2}^{1/2} dx\ x^n \exp(-ax^2). \tag{A2}$$

These integrals satisfy the recursion relation obtained by integration by parts valid for $n > 1$,

$$A_n = \frac{1}{2a}\left[(n-1)A_{n-2} - \frac{(-1)^n + 1}{2^{n-1}} \exp(-a/4) \right], \tag{A3}$$

where $A_1 = 0$ and A_0 is defined in Eq. (27). In the limit of large $|a|$, using the asymptotic expansions of the error function, we have

$$A_0(a) = \sqrt{\pi/a} + o(1/a^{3/2}) \quad \text{for } a \gg 1, \tag{A4}$$

$$A_0(a) = \exp(|a|/2)[1/|a| + o(1/|a|^2)] \quad \text{for } a \ll -1. \tag{A5}$$

Then using Eq. (A3), we find the result for the intensity fluctuations in a single polarization mode

$$\langle \Delta I_+^2 \rangle = \frac{I^2}{a} \quad \text{for } a \gg 1, \tag{A6}$$

$$\langle \Delta I_+^2 \rangle = \frac{I^2}{4} \quad \text{for } a \ll -1. \tag{A7}$$

When the cross saturation is neutral, the result is also simple. One has that $P(I_+)$ is flat, obtaining

$$\langle \Delta I_+^2 \rangle = \frac{I^2}{12} \quad \text{for } a = 0. \tag{A8}$$

The constant value obtained for $a \ll -1$ reflects the bimodal feature of the intensity distribution, which becomes more and more peaked around the circular polarization states as the cross-saturation asymmetry parameter δ increases in modulus. The width of each peak diminishes, but the total variance remains almost constant.

Calculating the same quantities in the restricted ensemble defined by Eq. (39), we find

$$\langle \Delta I_+^n \rangle_+ = I^n \sum_{k=0}^{n} \binom{n}{k} \frac{(-A_1')^{n-k} A_k'}{(A_0')^{n-k+1}}, \tag{A9}$$

where

$$A_n' = \int_0^{1/2} dx\, x^n \exp(-ax^2), \tag{A10}$$

and the new recursion relation for A_n' for $n > 1$ is given by

$$A_n' = \frac{1}{2a}\left[(n-1)A_{n-2}' - \frac{1}{2^{n-1}} \exp(-a/4) \right], \tag{A11}$$

with

$$A_0' = A_0/2,$$

$$A_1' = \frac{1}{2a}[1 - \exp(-a/4)]. \tag{A12}$$

Using these formulas for $n = 2$ and the asymptotic expansion of the complex error function, we obtain in the case $a \ll -1$

$$\langle \Delta I_+^2 \rangle_+ = I^2/|a|^2. \tag{A13}$$

APPENDIX B: MOMENTS OF TIME SCALES

Let us consider a process x obeying the Langevin equation

$$\dot{x} = F(x) + \sqrt{\epsilon}\xi. \tag{B1}$$

Then, using the Ito formalism, the correlation function $C(t) = \langle f(x(t)) f(x(0)) \rangle$ satisfies the equation of motion

$$\dot{C} = \langle f'(x(t)) F(x(t)) f(0) \rangle + \frac{\epsilon}{2} \langle f''(x(t)) f(x(0)) \rangle, \tag{B2}$$

where the prime indicates derivative with respect to x. Equation (B2) can be rewritten as $\dot{C} = \langle f(0) L f(t) \rangle$, introducing the linear operator L,

$$L = F(x)\frac{\partial}{\partial x} + \frac{\epsilon}{2}\frac{\partial^2}{\partial x^2}. \tag{B3}$$

Then the nth derivative of the correlation function can be expressed through successive applications of this evolution operator

$$\frac{d^n C(t)}{dt} = \langle f(0)(L^n f(t)) \rangle, \tag{B4}$$

where the abbreviation $f(t)$ stand for $f(x(t))$. To generalize the results of Ref. [45], we can use the equilibrium property

$$\langle L^n f^2(t) \rangle = 0 \tag{B5}$$

and we easily get

$$\lim_{t \to 0^+} \frac{d^n C}{dt^n} = -\langle f[L^n, f] \rangle, \tag{B6}$$

where the square brackets stand for the commutator.

In the case $n = 1$ we have

$$[L, f] = (Lf) + \epsilon f' \frac{\partial}{\partial x}. \tag{B7}$$

Using this result in Eq. (B6) we get

$$\lim_{t \to 0^+} \dot{C}(t) = -\frac{\epsilon}{2} \langle [f'(0)]^2 \rangle. \tag{B8}$$

which generalizes the result of Ref. [45] for a correlation function of functions of x.

[1] H. de Lang, Philips Res. Rep. Suppl. **8**, 1 (1967).
[2] D. Lenstra, Phys. Rep. **59**, 299 (1980).
[3] M. Sargent III, M. O. Scully, and W. E. Lamb, Jr., *Laser Physics* (Addison-Wesley, Reading, MA, 1974).
[4] D. Pohl, Appl. Phys. Lett. **20**, 266 (1972); N. M. Lawandy and R. S. Afzal, Opt. Commun. **65**, 452 (1988).
[5] J. Martin-Regalado, M. San Miguel, N. B. Abraham, and F. Prati, Opt. Lett. **21**, 351 (1996).
[6] J. Martin-Regalado, F. Prati, M. San Miguel, and N. B. Abraham, IEEE J. Quantum Electron. **33**, 765 (1997).
[7] J. Martin-Regalado, S. Balle, and M. San Miguel, Opt. Lett. **22**, 460 (1997).
[8] K. Otsuka, IEEE J. Quantum Electron. **QE-14**, 49 (1978); P. Besnard, X. Jia, R. Dalgliesh, A. D. May, and G. Stephan, J. Opt. Soc. Am. B **10**, 1605 (1996).
[9] A. Le Floch and R. LeNaour, Phys. Rev. A **4**, 290 (1971); F. Bretenaker, A. Le Floch, J. Davit, and J.-M. Chiquier, IEEE J. Quantum Electron. **28**, 348 (1992); P. Glorieux and A. Le Floch, Opt. Commun. **79**, 229 (1990).
[10] G. Stephan and D. Hugon, Phys. Rev. Lett. **55**, 703 (1985); A. D. May, P. Paddon, E. Sjerve, and G. Stephan, Phys. Rev. A **53**, 2829 (1996).
[11] G. P. Puccioni, M. V. Tratnik, J. E. Sipe, and G. L. Oppo, Opt. Lett. **12**, 242 (1987).
[12] A. P. Voitovich, L. P. Svirina, and V. N. Severikov, Opt. Commun. **80**, 435 (1991); L. Svirina, *ibid.* **111**, 370 (1994).

[13] T. Baer, J. Opt. Soc. Am. B **3**, 1175 (1986).
[14] X.-G. Wu and P. Mandel, J. Opt. Soc. Am. B **4**, 1870 (1987).
[15] K. Wiesenfeld, C. Bracikowski, G. James, and R. Roy, Phys. Rev. Lett. **65**, 1749 (1990); Q. Lue, N. Kugler, H. Weber, S. Dong, N. Mueller, and U. Wittrock, Opt. Quantum Electron. **28**, 57 (1996).
[16] E. Lacot, F. Stoeckel, and M. Chenevier, J. Phys. III **5**, 269 (1995); F. Sanchez, M. LeFlohic, G. M. Stephan, P. LeBoudec, and P.-L. Francois, IEEE J. Quantum Electron. **31**, 481 (1995).
[17] S. Bielawski and D. Derozier, J. Phys. III **5**, 251 (1995); S. Bielawski, D. Derozier, and P. Glorieux, Phys. Rev. A **46**, 2811 (1992).
[18] C. J. Chang-Hasnain, J. P. Harbison, G. Hasnain, A. C. Von Lehmen, L.T. Florez, and N. G. Stoffel, IEEE J. Quantum Electron. **27**, 1402 (1991); F. Robert, P. Besnard, M.-L. Chares, and G. M. Stephan, Opt. Quantum Electron. **27**, 805 (1995).
[19] A. K. Jansen van Doorn, M. P. van Exter, M. Travagnin, and J. P. Woerdman, Opt. Commun. **133**, 252 (1997); M. Travagnin, M. P. van Exter, A. K. Jansen van Doorn, and J. P. Woerdman, Phys. Rev. A **54**, 1647 (1996).
[20] M. D. Matlin, R. S. Gioggia, N. B. Abraham, P. Glorieux, and T. Crawford, Opt. Commun. **120**, 204 (1995); N. B. Abraham, M. D. Matlin, and R. S. Gioggia, Phys. Rev. A **53**, 3514 (1996).
[21] N. B. Abraham, E. Arimondo, and M. San Miguel, Opt. Commun. **117**, 344 (1995); **121**, 168 (1995).
[22] C. Serrat, A. Kul'minskii, R. Vilaseca, and R. Corbalan, Opt. Lett. **20**, 1353 (1995); A. Kul'minskii, R. Vilaseca, and R. Corbalan, *ibid.* **20**, 2390 (1995).
[23] C. Serrat, N. B. Abraham, M. San Miguel, R. Vilaseca, and J. Martin-Regalado, Phys. Rev. A **53**, R3731 (1996).
[24] C. A. Sharma, M. A. van Eijkelenborg, J. P. Woerdman, and M. San Miguel, Opt. Commun. **138**, 305 (1997).
[25] R. Graham, Phys. Lett. **103A**, 255 (1984).
[26] C. A. Schrama, M. A. van Eijkelenborg, and J. P. Woerdman, Opt. Commun. **132**, 557 (1996).
[27] S. Grossmann and W. Krauth, Phys. Rev. A **35**, 2523 (1987).
[28] W. Krauth and S. Grossmann, Phys. Rev. A **35**, 4192 (1987).
[29] V. I. Butkevich, V. E. Privalov, and M. M. Chervinskii, Opt. Spektrosk. **69**, 424 (1990) [Opt. Spectrosc. **69**, 252 (1990)].
[30] M. A. van Eijkelenborg, C. A. Schrama, and J. P. Woerdman, Opt. Commun. **119**, 97 (1995).
[31] J. P. Woerdman, M. A. van Eijkelenborg, M. P. van Exter, S. J. M. Kuppens, and C. A. Schrama, Quantum Semiclassic. Opt. **7**, 591 (1995).
[32] A. M. Lindberg, M. A. van Eijkelenborg, and J. P. Woerdman, IEEE J. Quantum Electron. (to be published).
[33] E. Goobar, J. W. Scott, B. Thibeault, G. Robinson, Y. Akulova, and L. A. Coldren, Appl. Phys. Lett. **67**, 3697 (1995); D. Kuksenkov, S. Feld, C. Wilmsen, H. Temkin, S. Swirhun, and R. Leibenguth, *ibid.* **66**, 277 (1995); D. V. Kuksenkov, H. Temkin, and S. Swirhun, *ibid.* **67**, 2141 (1995); J.-P. Zhang, IEEE J. Quantum Electron. **31**, 2127 (1995).
[34] M. Born and E. Wolf, *Principles of Optics*, 6th ed. (Pergamon, Oxford, 1993).
[35] H. De Lang, G. Bouwhuis, and E. T. Ferguson, Phys. Lett. **19**, 482 (1965); D. Polder and W. van Haeringen, Phys. Lett. **25A**, 337 (1967); W. van Haeringen, *ibid.* **24A**, 65 (1967).
[36] A. P. Voitovich, J. Sov. Laser Res. **8**, 574 (1987).
[37] C. H. Wang, W. J. Tomlinson, and R. T. George, Jr., Phys. Rev. **181**, 125 (1969); W. Culshaw, IEEE J. Quantum Electron. **QE-4**, 979 (1968); J. C. Cotteverte, F. Bretenaker, and A. Le Floch, Opt. Lett. **16**, 572 (1991).
[38] M. San Miguel, Q. Feng, and J. Moloney, Phys. Rev. A **52**, 1728 (1995).
[39] H. F. Hofmann and O. Hess, Phys. Rev. A (to be published).
[40] H. van Lem and D. Lenstra (unpublished).
[41] M. P. van Exter, R. F. M. Hendriks, and J. P. Woerdman (unpublished).
[42] A. K. Jansen van Doorn, M. P. van Exter, and J. P. Woerdman, Appl. Phys. Lett. **69**, 3635 (1996); M. P. van Exter, A. K. Jansen van Doorn, A. M. van der Lee, and J. P. Woerdman, Phys. Rev. A **55**, 1473 (1997).
[43] M. M. Tehrani and L. Mandel, Phys. Rev. A **17**, 679 (1978); S. Singh, Phys. Rep. **108**, 217 (1984); P. Lett and L. Mandel, J. Opt. Soc. Am. B **2**, 1615 (1985).
[44] L. Mandel and E. Wolf, *Optical Coherence and Quantum Optics* (Cambridge University Press, Cambridge, 1995).
[45] M. San Miguel, L. Pesquera, M. A. Rodriguez, and A. Hernandez-Machado, Phys. Rev. A **35**, 208 (1987).
[46] C. H. Wang and W. J. Tomlinson, Phys. Rev. **181**, 115 (1969).
[47] C. W. Gardiner, *Handbook of Stochastic Methods* (Springer-Verlag, Berlin, 1985).
[48] Note that when δ approaches 2, the intensity diverges because the nonlinear gain saturation terms in Eq. (1) are not sufficient to stabilize the intensity. We therefore consider strengths of the cross-saturation parameter that are much less than this limiting value.
[49] H. Risken, *The Fokker-Planck Equation* (Springer-Verlag, Berlin, 1989).
[50] In the marginal case $a=0$ we derive from Eq. (A8) that the condition of negligible partial intensity fluctuations is fulfilled if $I_0 \gg 12\epsilon/\alpha$.
[51] W. van Haeringen, Phys. Rev. A **158**, 256 (1967).